



Noise Figure and Gain Coefficient of Doped Fiber Amplifiers for Different Host Materials

Ahmed M. Emara, Yahya M. Zakaria, Moustafa H. Aly^{*}, Ali M. Okaz and Mahmoud S. Abou-El-Wafa
Department of Engineering Physics, Faculty of Engineering,
University of Alexandria, Egypt.
^{*} Member of the Optical Society of America (OSA).

Abstract

This paper provides a numerical investigation of the noise performance of erbium doped fiber amplifiers (EDFAs) and praseodymium doped fiber amplifiers (PDFAs) in different types of host materials. The noise figure and gain coefficient are calculated for different values of pump and signal wavelengths and optimum operational conditions are established for using the amplifiers in optical communication systems.

I. INTRODUCTION

Rare-earth doped fiber amplifiers have revolutionized optical fiber communications as well as other scientific disciplines [1-5]. The technique of doping silica fibers with elements such as erbium, praseodymium and thulium allows an exempt gain medium that can be pumped optically to make lasers and amplifiers. Trivalent rare-earth elements are the only ions for which lasing transitions are observed in silica hosts. Two of these transitions (near 1.31 μm and 1.55 μm) are suitable for the transmission windows of optical communication.

Optical amplifiers operating around 1.3 μm are of great interest since a substantial part of the fiber network worldwide (~50 million kilometers) is designed to perform at the second telecommunication window (~1.31 μm) at which minimum dispersion is observed in silica fibers. Fiber amplifiers with praseodymium ion (Pr^{3+}) dopant in fluorozirconate host glasses have demonstrated commending results at wavelengths covering this window and praseodymium-doped fiber amplifiers (PDFAs) are now the subject of intense research efforts [6-9]. More established are the erbium-doped fiber amplifiers (EDFAs), which are widely used in the third telecommunication window around 1.55 μm , corresponding to the lowest losses in silica fibers [1, 9]. However, the performance of an EDFA depends strongly on the host glass and a stable performance in a certain material is possible only when all the operating conditions are considered.

The host material dictates the performance through the values of its absorption and emission cross sections for the transmitted photons. These cross-sections have an inherent dependence on the signal wavelength. However, the reliance of the noise figure and gain coefficient on the cross sections is of complex nature and a thorough analysis is necessary to characterize the amplifier performance. An efficient optical amplifier is characterized by high gain coefficient, low noise figure and wide bandwidth. A high gain coefficient will ascertain longer transmission distances without the need to re-amplify the signal. A low noise figure is necessary prerequisite for the fidelity of the transmission system.

This paper compares the performance of EDFAs and PDFAs from the noise figure point of view. The noise figure shows the effect of the amplifier on the signal to noise ratio (SNR), which must be high enough for proper detection of the signal at the receiving end. EDFAs are studied when two types of alumino-germanosilicate



glass hosts for the Er^{3+} ions are used. PDFAs are studied for Pr^{3+} -doped ZBLAN fiber amplifiers. Numerical calculations are performed to establish the parametric dependence of the amplifier gain and noise figure on both the transmitted signal and optical pump wavelengths. In Section II, the theoretical model for noise calculations in case of a three-level laser system is described. Section III summarizes the results obtained for the noise figure and gain coefficient for both EDFAs and PDFAs. The conclusions are given in Section IV.

II. THEORY

The energy level diagrams of erbium and praseodymium are shown in Fig. 1 and Fig. 2, respectively. It is obvious that optical signals at wavelength $1.31 \mu m$ can be amplified using Pr-doping because of its ${}^1G_4 \rightarrow {}^3H_5$ lasing transition. Signals at wavelength $1.55 \mu m$ can be amplified using Er-doping using its ${}^4I_{13/2} \rightarrow {}^4I_{15/2}$ transition.

In calculating the gain coefficient and the noise figure, both Er^{3+} and Pr^{3+} are considered as three-level laser systems. Figure 3 represents the different possible transitions associated with absorption or emission of one photon from photon number state $|n\rangle$. The probability $P_{l,k;j,\ell}$ represents the change in photon number due to either emission ($i=1, j=2$) or absorption ($i=2, j=1$) between photon number states $|l\rangle$ and $|k\rangle$.

When a signal of intensity I_s and wavelength λ_s traverses a medium of thickness dz and atomic populations of N_1, N_2 in the lower and upper energy levels, respectively, the change in the photon number probability dP_n is given by:

$$\frac{dP_n}{dz} = \sigma_a N_1 (P_{2,n+1,n+1} - P_{2,n-1,n-1}) + \sigma_e N_2 (P_{1,n+2,n-1} - P_{1,n-1,2,n}). \quad (1)$$

By averaging over the coordinate z and using the relation between the transition probability and signal intensity, the following relation is obtained for the intensity change dI_s :

$$\begin{aligned} dI_s &= [\sigma_e(\lambda_s)N_2 - \sigma_a(\lambda_s)N_1]I_s dz \\ &= gI_s dz, \end{aligned} \quad (2)$$

with g the gain coefficient, σ_e and σ_a the emission and absorption cross sections, respectively. The gain coefficient depends on the signal wavelength and the relative medium inversion D and is related to the gain coefficient by [1]:

$$g = \frac{\rho[\sigma_e(\lambda_s)(1+D) - \sigma_a(\lambda_s)(1-D)]}{2} \quad (3)$$

where $D = (N_2 - N_1) / \rho$, ρ being the density of the rare earth ions in the core. The emission and absorption cross sections of praseodymium and erbium in different host glass materials, necessary for applying Eq. (3), has been measured experimentally [8, 10, 11].

For digital communication systems, the signal input to the amplifier with mean $\langle n(0) \rangle$ is actually modulated in time, frequency or phase for conveying information at a bit rate $B=1/T$, with T the bit period. At the amplifier output, the quantity $\langle n(z) \rangle_{ASE}$ ($= M N(z)$, where M is the number of possible transmitted modes and $N(z)$ is the amplified spontaneous emission (ASE) noise photon number) is defined as the unmodulated background ASE noise. Therefore, the quantity given by $\langle n(z) \rangle - \langle n(z) \rangle_{ASE}$ represents the mean photon number that contains signal information. At the receiving end, the modulated signal power $P_{sig} \approx \langle n(z) \rangle - \langle n(z) \rangle_{ASE}$ is converted into photocurrent, with an electrical power $P_{phot} \approx (P_{sig})^2$. On the other hand, the associated noise power is $P_{noise} \approx \sigma^2$ (where σ is the variance).

The optical signal to noise ratio (SNR_o) is defined by [1]:

$$SNR_o(z) = \frac{\langle \langle n(z) \rangle - \langle n(z) \rangle_{ASE} \rangle_T^2}{\sigma^2(z)} = \frac{G^2(z) \langle n(0) \rangle^2}{\sigma^2(z)} \quad (4)$$

where $\langle \cdot \rangle_T$ indicates time average over the bit period and G is the amplifier gain. For input signals with Poisson statistics, we have $\sigma^2(0) = \langle n(0) \rangle$, and the $SNR_o(0)$ is equal to the mean, i.e.,

$$SNR_o(0) = \langle n(0) \rangle. \quad (5)$$

But the mean and variance of the photon number are given by [1]:

$$\langle n(z) \rangle = G(z)\langle n(0) \rangle + MN(z), \quad (6-a)$$

and

$$\sigma^2(z) = G^2(z)[\sigma^2(0) - \langle n(0) \rangle] + G(z)\langle n(0) \rangle + MN(z) + 2G(z)\langle n(0) \rangle N(z) + MN^2(z). \quad (6-b)$$

Thus, if we have for Poisson statistics:

$$\frac{1}{SNR_o(z)} = \frac{1}{\langle n(0) \rangle} \left[\frac{1 + 2N(z)}{G(z)} + \frac{MN(z)[N(z) + 1]}{G^2(z)\langle n(0) \rangle} \right], \quad (7)$$

the amplifier optical noise figure $F_o(z)$ is:

$$F_o(z) = \frac{SNR_o(0)}{SNR_o(z)}, \quad (8)$$

where $SNR_o(0)$ is the amplifier input optical SNR, the optical noise figure represents a measure of the SNR_o degradation experienced by the signal after passing through the amplifier. As the amplifier introduces noise, it is expected that $SNR_o(z) < SNR_o(0)$, so the optical noise figure is always greater than or equal to unity. Then the optical noise figure becomes:

$$F_o(z) = \frac{1 + 2N(z)}{G(z)} + \frac{MN(z)[N(z) + 1]}{G^2(z)\langle n(0) \rangle}. \quad (9)$$

If we assume an input power high enough such that $G \langle n(0) \rangle \gg N$, and in the high gain limit $G \gg 1$, then from Eqs. (5), (8) and (9), the optical noise figure reduces to:

$$F_o(z) = 2n_{sp}(z), \quad (10)$$

where $n_{sp}(z)$ is the spontaneous emission factor, given by:

$$n_{sp}(z) = \frac{N(z)}{G(z) - 1}. \quad (11)$$

This spontaneous emission factor is always greater than or equal to unity (for complete medium inversion), so the noise figure of the high gain amplifier is always greater than 2 corresponding to $F_o > 3\text{dB}$.

For high pump powers, the minimum spontaneous emission factor can be derived as:

$$n_{sp}^{\min}(\lambda_p, \lambda_s) = \frac{1}{1 - \frac{\sigma_e(\lambda_p)\sigma_s(\lambda_s)}{\sigma_a(\lambda_p)\sigma_e(\lambda_s)}}, \quad (12)$$

where λ_p and λ_s are the pump and the signal wavelengths, respectively. The minimum amplifier noise figure is given by:

$$F_o^{\min}(\lambda_p, \lambda_s) = \frac{2}{1 - \frac{\sigma_e(\lambda_p)\sigma_s(\lambda_s)}{\sigma_a(\lambda_p)\sigma_e(\lambda_s)}}. \quad (13)$$

For an EDFA pumped as a three-level system, we have $\sigma_e(\lambda_p) = 0$. Thus $F_o^{\min} = 3\text{dB}$. The 3dB lower limit obtained for the optical noise figure at high gain is called the quantum limit. The quantum limit condition $F_o \geq 2$ only applies to the case of high gain amplifiers, on the other hand for low gain amplifiers the noise figure can be such that $1 \leq F_o \leq 2$. For cases where $\sigma_e(\lambda_p) \neq 0$, the minimum achievable noise figure is always $> 3\text{dB}$.

III. RESULTS

To check our model, calculations are made for an EDFA in a germanosilicate glass host, whose data is already published [1]. The reported absorption and emission cross sections and the minimum noise figure, calculated



using Eq. (13), were reproduced. The results depicted in Fig. 4 and Fig. 5 show complete agreement with the published data.

Then the reported cross sections of two other EDFA silica hosts were used in our computational model. The materials are both alumino-germanosilicate glasses with type (B) characterized by a higher concentration of Al-dopant than type (A). Figure 6 shows the absorption and emission cross sections for EDFA in a type A material, while Fig. 7 shows the minimum noise figure calculated at different values for the pump and signal wavelengths. The minimum noise figure was found to be 4.085 dB at a signal wavelength 1.535 μm and pump wavelength 1.475 μm . Similar data for type (B) glass host are shown in Fig. 8 Fig. 9. Type (B) shows that the minimum noise figure is 4.393 dB at signal wavelength 1.546 μm and a pump wavelength 1.475 μm . Based on these figures, type (A) is recommended from the noise considerations point of view only.

Calculations are also made for PDFA hosted in a ZBLAN glass. Figure 10 shows the reported absorption and emission cross sections [8] and [10]. The calculated minimum noise figure in Figure 11 is 3.031 dB at a signal wavelength 1.31 μm and a pump wavelength 1.015 μm . Fig. 12 shows a projection of the PDFA noise figure at $\lambda_p = 1.08 \mu\text{m}$. It agrees with the general experimental behaviour reported recently [12]. The differences in the noise figure values may be attributed to the low pump power used in the aforementioned reference and not covered by the present analysis. Generally, it could be seen that the noise levels associated with PDFA are similar to those reported with EDFAs, though it should be mentioned that both amplifiers are normally utilized at different wavelengths.

In Fig. 13 the gain coefficient, based on Eq. (3), is plotted for different values of the relative medium inversion D . The plots range from $D = -1$ which means that all ions are in the ground state to $D = +1$ corresponding to the case where all ions are in an excited state. For all calculations, the density of the rare-earth ions in the core are assumed to be $1 \times 10^{25} \text{ m}^{-3}$. From Fig. 13, it is obvious that when all ions are in the ground state, the medium acts purely as an absorbing medium. This is pronounced by the negative values of the gain coefficient. As D increases the region of positive gain coefficient becomes more prominent. This is to be compared with the case when all ions are in the excited state. At this case, the medium is totally amplifying characterized by 100% positive gain coefficient. It can be noticed generally that the gain coefficient for EDFA is greater than that of PDFA. However, PDFA shows a broader band of positive gain coefficient though we need to reassert that the two amplifiers operate at different transmission windows. The gain coefficient is maximum at 1.54 μm for Er and 1.31 μm for Pr.

IV. CONCLUSIONS

The noise performance of EDFAs and PDFAs has been calculated. The noise figure shows a strong dependence on the pump and signal wavelengths as well as on the host glass. Its minimum values are 4.085 dB for alumino-germanosilicate glass, type (A), material, and 4.393 dB for alumino-germanosilicate glass, type (B). The first figure is better than the most recent reported average value of 4.3 dB [13]. As for PDFA in ZBLAN glass, the minimum noise figure is 3.031 dB at 1.31 μm , which is by far superior to the recently quoted measurement of 6.6 dB [11]. The gain coefficient is maximum at 1.54 μm for Er^{3+} and 1.317 μm for Pr^{3+} .

REFERENCES

- [1] E. Desurvire, Erbium-Doped Fiber Amplifiers: Principles and Applications, John Wiley, New York, 1994.
- [2] D. N. Payne, "Optical amplifiers – A telecommunications revolution," Proc. EPSRC ITEC '96, pp. 29–30, October 1996.



- [3] S. D. Jackson and T. A. King, "CW operation of a 1.064- μm pumped Tm-Ho-doped silica fiber laser," *IEEE J. Quantum Electron.*, Vol. 34, No. 9, pp. 1578-1587, 1998.
- [4] E. R. M. Taylor, B. N. Samson, M. Naftaly, A. Jha and D. N. Payne, "A 1300nm Nd³⁺-doped glass amplifier," *Proc. ECOC'98, Madrid, Spain, Sep. 20-24, 1998.*
- [5] H. M. Pask, A. C. Tropper and D. C. Hanna, "A Pr³⁺-doped ZBLAN fibre upconversion laser pumped by an Yb³⁺-doped silica fibre laser," *Opt. Comms.*, Vol. 134, No. 1-6, pp. 139-144, 1997.
- [6] Y. Durteste, M. Monerie, J. Y. Allain and H. Poignant, "Amplification and lasing at 1.3- μm in praseodymium-doped fluorozirconate fibers," *Electron. Lett.*, Vol. 27, No. 8, pp. 626-628, 1991.
- [7] S. C. Fleming, "Crosstalk in 1.3 μm praseodymium fluoride fiber amplifiers," *J. Lightwave Technol.*, Vol. 14, No. 1, pp. 66-71, 1996.
- [8] B. Pedersen, W. J. Miniscalco and R. S. Quimby, "Optimization of Pr³⁺: ZBLAN fiber amplifiers," *Photon Technol. Lett.*, Vol. 4, No. 5, pp. 446-48, 1992.
- [9] P. Myslinski, D. Nguyen and J. Chrostowski, "Effects of concentration on the performance of erbium-doped fiber amplifiers," *J. Lightwave Technol.*, Vol. 15, No. 1, pp. 112-120, 1997
- [10] W. L. Barnes, R. I. Laming, E. J. Tarbox and P. R. Morkel, "Absorption and emission cross section of Er³⁺ doped silica fibers," *IEEE J. Quantum Electron.*, Vol. 27, No. 4, pp. 1004-1010, 1991.
- [11] Y. Nishida, M. Yamada, T. Kanamori, K. Kobayashi, J. Temmyo, S. Sudo and Y. Ohishi, "Development of an efficient praseodymium-doped fiber amplifier," *IEEE J. Quantum Electron.*, Vol. 34, No. 8, pp. 1332-1339, 1998.
- [12] K. Nakazato, C. Fakuda, M. Onishi and M. Nishimara, "Performance of Pr-doped fiber fluoride amplifier for multichannel AM-VSB transmission", *Electron. Lett.*, Vol.29, No. 18, 1993.
- [13] M. Movassaghi, M. K. Jackson, V. M. Smith and W. J. Hallam, "Noise figure of erbium-doped fiber amplifiers in saturated operation", *J. Lightwave Technol.*, Vol. 16, No. 5, pp. 812-817, 1998.

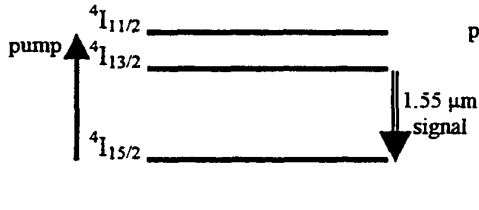


Fig. 1. Energy levels of Er^{3+} .

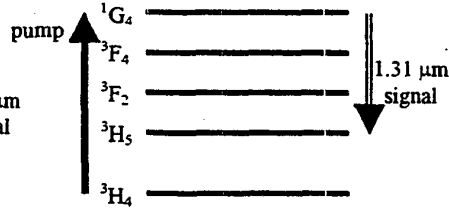


Fig. 2. Energy levels of Pr^{3+} .

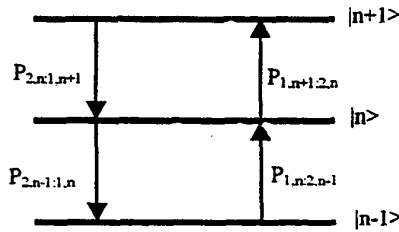


Fig. 3. Transition probabilities associated with photon number state $|n\rangle$.

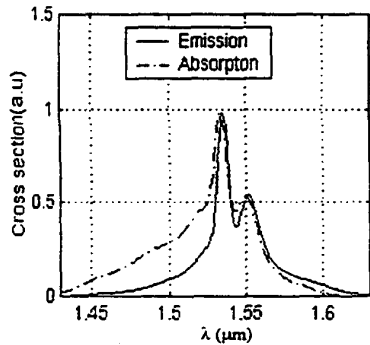


Fig. 4. Absorption and emission cross section of Er^{3+} in germanosilicate glass.

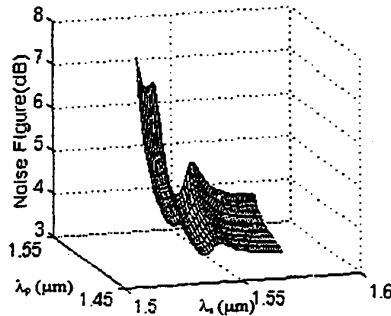


Fig. 5. Noise figure of Er^{3+} in germanosilicate glass.

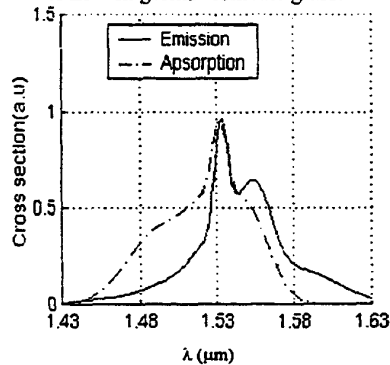


Fig. 6. Absorption and emission cross section of Er^{3+} in aluminogermanosilicate glass type (A).

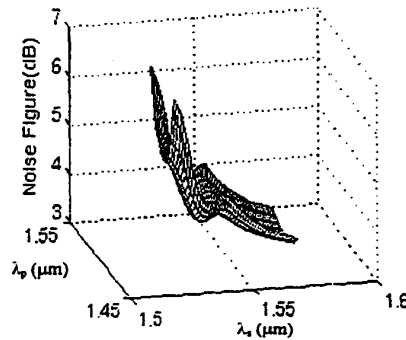


Fig. 7. Noise figure of Er^{3+} in aluminogermanosilicate glass type (A).

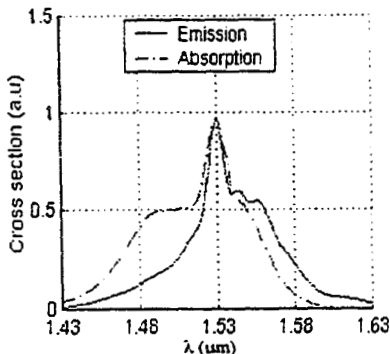


Fig. 8. Absorption and emission cross section of Er^{3+} in aluminogermanosilicate glass type (B).

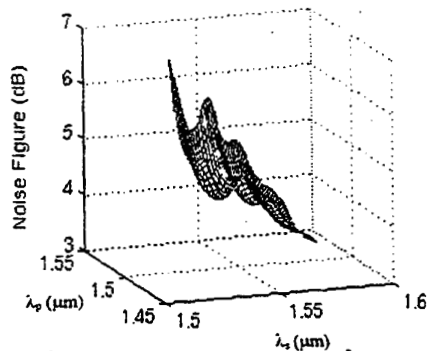


Fig. 9. Noise figure of Er^{3+} in aluminogermanosilicate glass type (B).

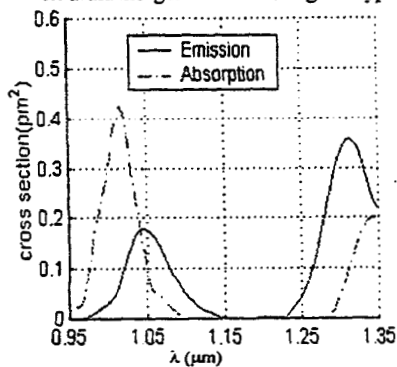


Fig. 10. Absorption and emission cross section of Pr^{3+} in ZBLAN.

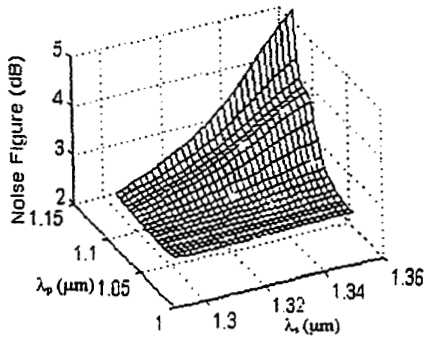


Fig. 11. Noise figure of Pr^{3+} in ZBLAN.

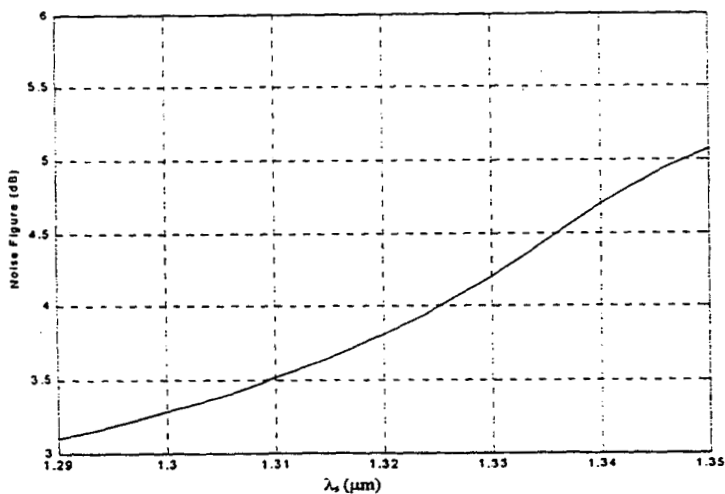


Fig. 12 Noise figure of Pr^{3+} in ZBLAN at 1.08 μm pump wavelength.

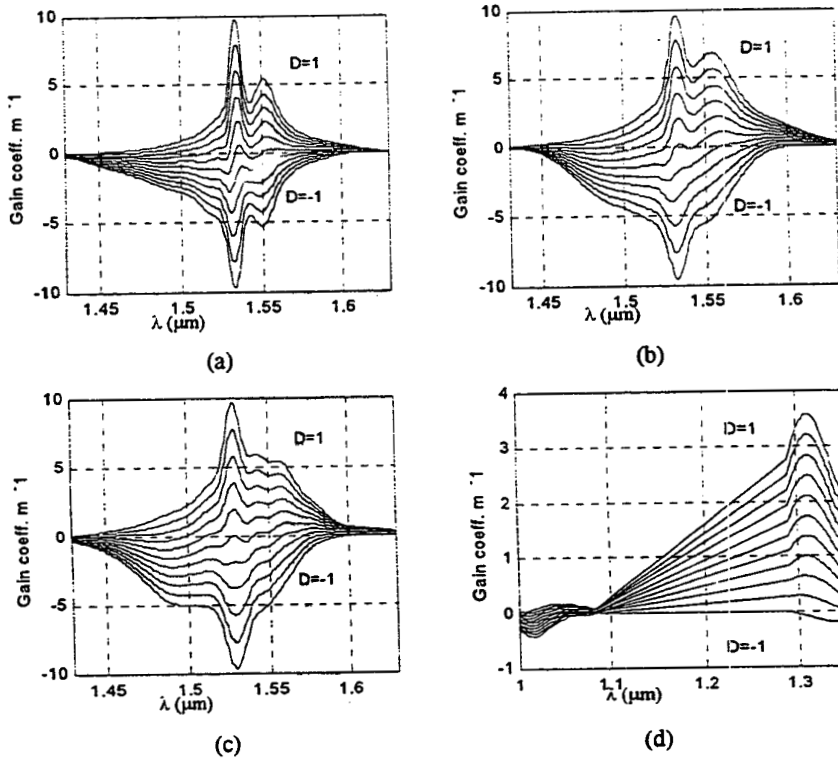


Fig. 13. Gain coefficient of Er^{3+} and Pr^{3+} in different host materials:
 (a) Er^{3+} in germanosilicate glass, (b) Er^{3+} in alumino-germanosilicate glass type (A),
 (c) Er^{3+} in alumino-germanosilicate glass type (B), (d) Pr^{3+} in ZBLAN.